US006377832B1

(12) **United States Patent**
Bergman et al.

(10) **Patent No.: US 6,377,832 B1**
(45) **Date of Patent: *Apr. 23, 2002**

(54) **SYSTEM AND METHOD FOR ANALYZING A MEDICAL IMAGE**

(75) Inventors: **Harris L. Bergman**, Smyrna; **David N. Ku**, Atlanta, both of GA (US)

(73) Assignee: **Georgia Tech Research Corporation**, Atlanta, GA (US)

(*) Notice: This patent issued on a continued prosecution application filed under 37 CFR 1.53(d), and is subject to the twenty year patent term provisions of 35 U.S.C. 154(a)(2).

Subject to any disclaimer, the term of this patent is extended or adjusted under 35 U.S.C. 154(b) by 0 days.

(21) Appl. No.: **09/272,862**

(22) Filed: **Mar. 19, 1999**

Related U.S. Application Data

(60) Provisional application No. 60/078,811, filed on Mar. 20, 1998.

(51) **Int. Cl.**[7] **A61B 5/05**

(52) **U.S. Cl.** **600/408**; 600/410; 128/925

(58) **Field of Search** 600/408, 410, 600/411, 425, 427; 128/920, 922, 923, 924, 925

(56) **References Cited**

U.S. PATENT DOCUMENTS

4,849,697	A	* 7/1989	Cline et al.	324/306
5,150,292	A	* 9/1992	Hoffmann et al.	600/420
5,190,744	A	* 3/1993	Rocklage et al.	424/9
5,352,979	A	* 10/1994	Conturo	324/307
5,377,681	A	* 1/1995	Drane	600/419
5,638,823	A	* 6/1997	Akay et al.	600/504
5,685,305	A	* 11/1997	Moonen et al.	600/419
5,872,861	A	* 2/1999	Makram-Ebeid	382/130

OTHER PUBLICATIONS

A. Armoni, "Use of Neutral Networks in Medical Diagnoses," M.D. Computing, vol. 15, No. 2, 1998, pp. 100–104.
Perman, et al., "Artifacts from Pulsatile Flow in MR Imaging," Journal of Computer Assisted Tomography, vol. 10, No. 3, 1986, pp. 475–483.
Downing, et al, "Flow Through a Compliant Stenotic Artery," Advances in Bioengineering, vol. 26, 1993, pp. 137–140.
Barnett, et al., "Beneficial Effect of Carotid Endarterectomy in Symptomatic Patients with High–Grade Carotid Stenosis," The New England Journal of Medicine, vol. 325, No. 7, Aug. 15, 1991, pp. 445–453.
Scarselli, et al., Universal Approximation using Feedforward Neural Networks: a Survey of Some Existing Methods, and Some New Results, Neural Networks, vol. 11, No. 1, 1998, pp. 15–37.
Saloner, et al., "MRA Studies of Aterial Stenosis: Improvements by Diastolic Acquisition," MRM 31 1994, pp. 196–203.

(List continued on next page.)

Primary Examiner—Brian L. Casler
(74) *Attorney, Agent, or Firm*—Thomas, Kayden, Horstemeyer & Risley LLP

(57) **ABSTRACT**

Disclosed is a system and method for determining a severity of a stenosis in a blood vessel depicted in a magnetic resonance imaging (MRI) data set. The system comprises a neural network configured to calculate the severity of the stenosis in the blood vessel based upon a number of input parameters, and the input parameters including at least one characteristic of a signal void associated with the stenosis in the MRI data set. The input parameters may include, for example, a flow rate of blood through the blood vessel, a length of a longitudinal axis of the signal void, and an average image intensity along the longitudinal axis of the signal void as well as other input parameters.

80 Claims, 7 Drawing Sheets

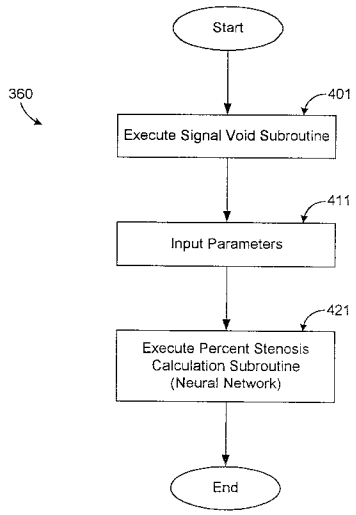

OTHER PUBLICATIONS

Scott Sheppard, MS, "Basic Concepts in Magnetic Resonance Angiography," Radiologic Clinics of North America, vol. 33, No. 1, Jan. 1995, pp. 91–112.

Masaryk, et al., "Carotid Bifurcaction: MR Imaging Work in Progress," Radiology, vol. 166, No. 2, Feb. 1988 pp. 461–466.

Tsuruda, et al., "Artifacts Associated with MR Neuroangiography," Americal Society of Neuroadiology, ANJR: 13, Sep./Oct. 1992, pp. 1411–1422.

Young, et al., "Flow Characteristics in Models of Arterial Stenoses–I. Steady Flow," J. Biomechanics, 1973, vol. 6, No. 4–E, pp. 395–410.

Kim, et al., Experimental Measurements of Turbulence Spectra Distal to Stenoses, J. Biomechanics, 1974, vol. 7, pp. 335–342.

C.Clark, "Turbulent Velocity Measurements in a Model of Aortic Stenosis," J. Biomechanics, 1976, vol. 9, pp. 677–687.

Soh, et al., "Laminar Entrance Flow in a Curved Pipe," J. Fluid Mech., 1984, vol. 148, pp. 109–135.

Gatenby, et al., "Mapping of Turbulent Intensity by Magnetic Resonance Imaging," Journal of Magnetic Resonance, Series B 104, 1994, pp. 119–126.

Oshinski, et al., Turbulent Fluctuation Velocity: The Most Significant Determinant of Signal Loss in Stenotic Vessels, MRM 33: 193–199, 1995.

Siegel, et al., "Computational Simulation of Turbulent Signal Loss in 2D Time–of–Flight Magnetic Resonance Angiograms," MRM 37:609–614, 1997.

Kuethe, et al., NMR Signal Loss from Turbulence: Models of Time Dependence Compared with Data, The American Physical Society, 1995, pp. 3252–3261.

Gatenaby, et al., "Characterization of Turbulent Flows by NMR Measurements with Pulsed Gradients," Journal of Magnetic Resonance, Series A 110, 1994, pp. 26–32.

Gao, et al., "Turbulent Flow Effects on NMR Imaging: Measurement of Turbulent Intensity," Med. Phys. vol. 18 No. 5, Sep./Oct. 1991, pp. 1045–1051.

Rittgers, et al., "Velocity Profiles in Stenosed Tube Models Using Magnetic Resonance Imaging," Transactions of the ASME, vol. 110, Aug. 1988, pp. 180–184.

Tyen, et al., "MR Imaging of Flow Through Tortuous Vessels: A Numerical Simulation," MRM 31:184–195, (1994).

Dean O. Kuethe, "Measuring Distributions of Diffusivity in Turbulent Fluids with Magnetic–Resonance Imaging," The American Physical Society, vol. 40, No. 8, pp. 4542–4551.

Urchuk, et al., "Mechanisms of Flow–Induced Signal Loss in MR Angiography," JMRI 1992; 2:453–462.

Spielmann, et al., "Appearance of Poststenotic Jets in MRI: Dependence on Flow Velocity and on Imaging Parameters," Magnetic Resonance Imaging, vol. 9, pp. 67–72, 1991.

Krug, et al., "MR Imaging of Poststenotic Flow Phenomena: Experimental Studies," JMRI 1991: 1:585–591.

Gatenby, et al., "Mechanisms of Signal Loss in MR Imaging of Stenoses," SMRM 1992, p. 2814.

Frank, et al., "Distortions from Curved Flow in Magnetic Resonance Imaging," 1993, pp. 84–93.

Gatenby, et al., "An Investigation Using Partial Echo Techniques of Post–Stenotic Signal," SMRM 1991, p. 364.

Evans, et al., "Effects of Turbulence on Signal Intensity in Gradient Echo Images," Investigative Radiology, vol. 23, Jul. 1988, pp. 512–518.

P.G. De Gennes, "Theory of Spin Echos in a Turbulent Fluid," Physics Letters, vol. 29A, No. 1, Mar. 1969, pp. 23–24.

Bradley, Jr., et al., "The Appearance of Rapidly Flowing Blood on Magnetic Resonance Images," AJR: 143, Dec. 1964, pp. 1167–1174.

Bradley, et al., "Blood Flow: Magnetic Resonance Imaging," Radiology 1985: 154: 443–450.

Gatenby, et al., "Echo–Planar–Imaging Studies of Turbulent Flow," Journal of Magnetic Resonance, Series A 121, 1996, pp. 193–200.

Li, et al., "Turbulent Pipe Flow studied by Time–Averaged NMR Imaging: Measurements of Velocity Profile and Turbulent Intensity," Magnetic Resonance Imaging, vol. 12, No. 6, pp. 923–934.

Maclin, et al., How to Improve a Neural Network for Early Detection of Hepatic Cancer, Cancer Letters, 77, 1994, pp. 95–101.

Ouyang, et al., "Using a Neural Network to Diagnose the Hypertonic Portions of Hypertonic Cardiomyopathy," M.D. Computing, vol. 15, No. 2, 1998, pp. 106–109.

Adi Armoni, Ph.D., "Use of Neural Networks in Medical Diagnosis," M.D. Computing, vol. 15, No. 2, 1998, pp. 100–104.

Hal S. Stern, Technologies, vol. 38, No. 3, Aug. 1996, pp. 205–213.

Nishimura, et al., "On the Nature and Reduction of the Displacement Artifact in Flow Images," Magnetic Resonance in Medicine, 22, 1991, pp. 481–492.

Garbini, et al., Measurement of Fluid Turbulence Based on Pulsed Ultrasound Techniques, Part 1, Analysis, J. Fluid Mech., vol. 118, 1982, pp. 445–470.

Garbini, et al., "Measurement of Fluid Turbulence Based on Pulsed Ultrasound Techniques, Part 2, Experimental Investigation," J. Fluid Mech. vol. 118, 1982, p. 471–505.

Goodenday, et al., "Identifying Coronary Stenosis Using an Image–Recognition Neural Network," IEEE Engineering in Medicine and Biology, Sep./Oct. 1997, pp. 139–144.

Coppini, et al., "A Neural Network Architecture for Understanding Discrete Three–Dimensional Scenes in Medical Imaging," Computers and Biomedical Research 25, 1992, pp. 569–585.

Fredfelt, et al., "Automatic Screening of Plain Film Mammography," Seminars in Ultrasound, CT, and MRI, vol. 13, No. 2, Apr. 1992, pp. 135–139.

Nekovei, et al., "Back–Propagation Network and its Configuration for Blood Vessel Detection in Angiograms," IEEE Transactions on Neural Networks, vol. 6, No. 1, Jan. 1995, pp. 64–72.

Cios, et al., "Neural Networks in Detection of Coronary Artery Disease," IEEE, 1990, pp. 33–37.

Gao, et al., "Nuclear Magnetic Resonance Signal from Flowing Nuclei in Rapid Imaging Using Gradient Echos," Med. Phys., 15(6), Nov./Dec. 1988, pp. 809–814.

Yuan, et al., "The Solution of Bloch Equations for Flowing Spins During a Selective Pulse Using a Finite Difference Method," Med. Phys, 14(6), Nov./Dec. 1987, pp. 914–921.

Caprihan, et al., "Flow Measurements by NMR," Physics Reports, 198, No. 4, 1990, pp. 195–235.

Doi, et al., "Computer–Aided Diagnosis: Development of Automated Schemes for Quantitative Analysis of Radiographic Images," Seminars in Ultrasound, CT, and MRI, vol. 12, No. 2, Apr. 1992, pp. 140–152.

Duerk, et al., "Experimental Confirmation of Phase Encoding of Instantaneous Derivatives of Position," MRM 32:77–87, 1994.

Dumoulin, et al., "Noninvasive Measurement of Renal Hemodynamic Functions using Gadolinium Enhanced Magnetic Resonance Imaging," MRM 32:370–378, 1994.

Simonetti, et al., "Significance of the Point of Expansion in Interpretation of Gradient Moments and Motion Sensitivity," JMI, vol. 1, No. 5, Sep./Oct. 1991, pp. 569–576.

Schmallbrock, et al., "Volume MR Angiography: Methods to Achieve Very Short Echo Times," Radiology, vol. 175, No. 3, Jun. 1990, pp. 861–865.

Fukuda, et al., "Transition from Laminar to Turbulent Flow of Water in a Pipe Measured by a Pulsed NMR Method," Journal of the Physical Society of Japan, vol. 54, No. 2, Dec. 1985, pp. 4555–4560.

Fukuda, et al., "A Pulsed NMR Study on the Flow of Fluid," Journal of Physical Society of Japan, vol. 47, No. 6, Dec. 1979, pp. 1999–2006.

de Roos et al., Cine MR imaging in aortic stenosis, J Comp Assist Tomogr 13(3): 421–5, 1989 May–Jun.*

Mirowitz et al., Normal signal–void patterns in cardiac cine MR images, Radiology 176(1): 49–55, 1990 Jul.*

* cited by examiner

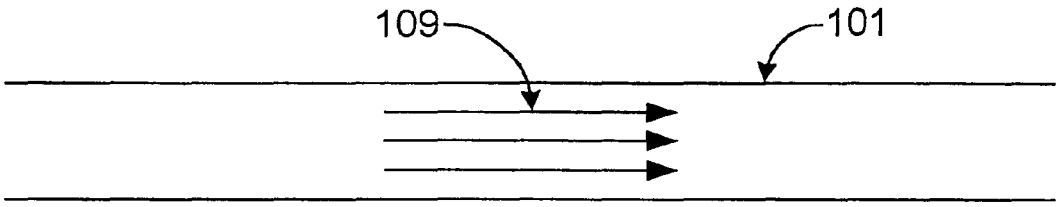

Fig. 1A

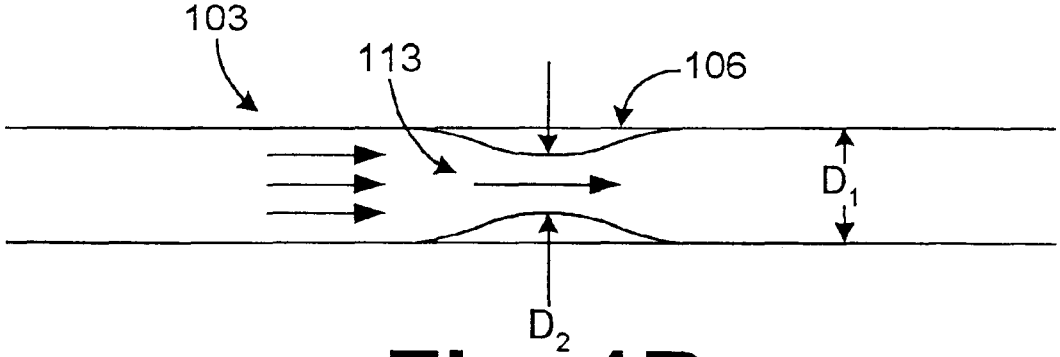

Fig. 1B

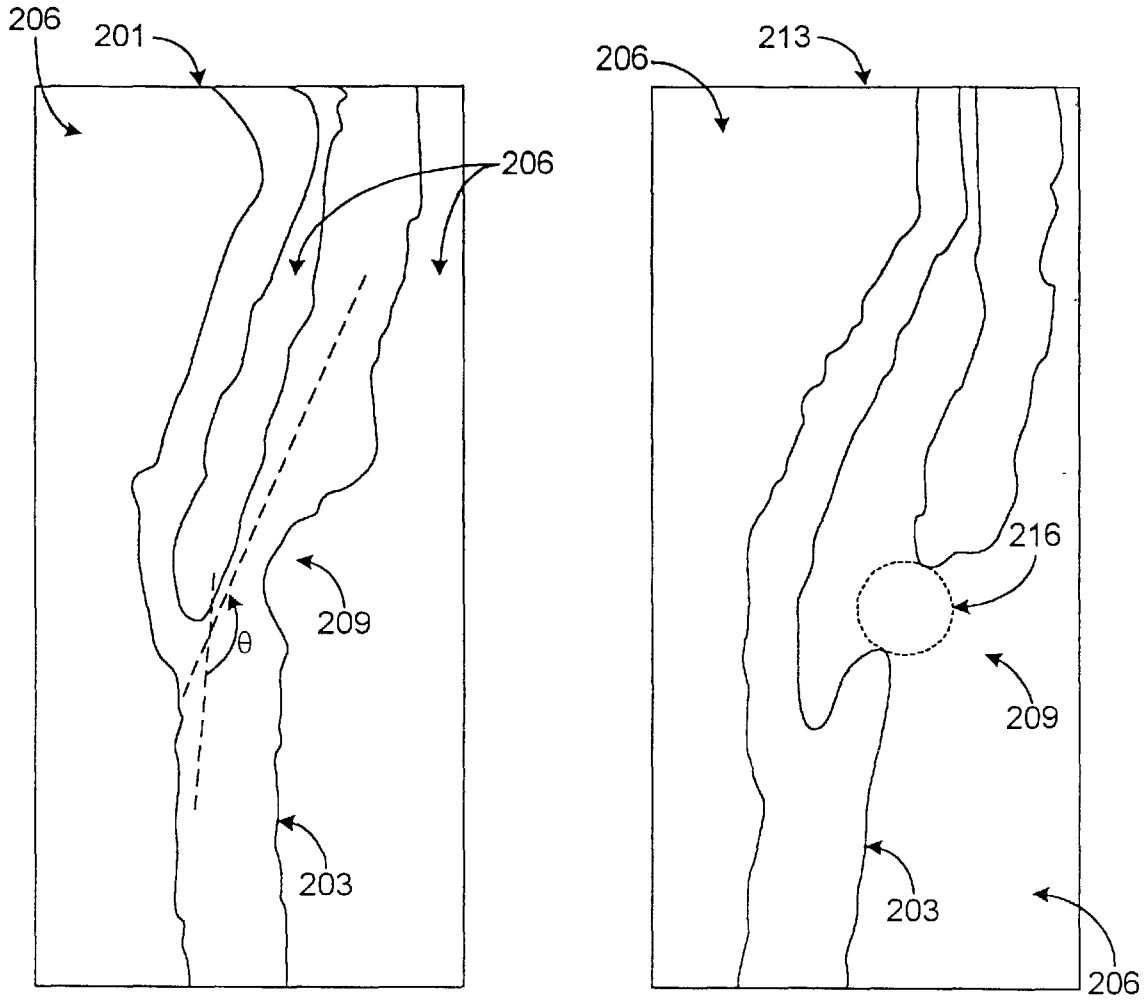

Fig. 2

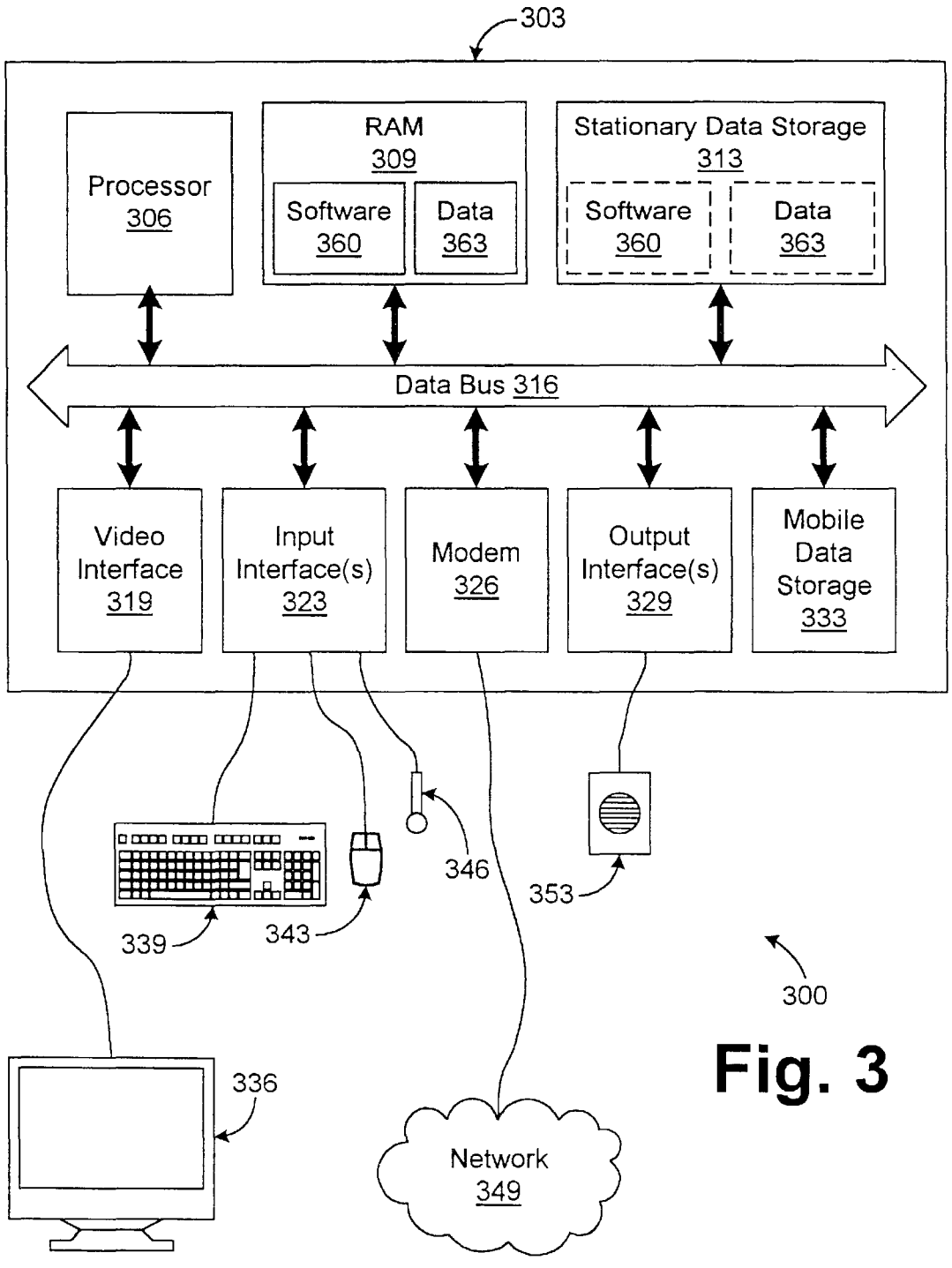
303
Processor
306
RAM
309
Software
360
Data
363
Stationary Data Storage
313
Software
360
Data
363
Data Bus 316
Video
Interface
319
Input
Interface(s)
323
Modem
326
Output
Interface(s)
329
Mobile
Data
Storage
333
339
343
346
353
336
Network
349
300

Fig. 3

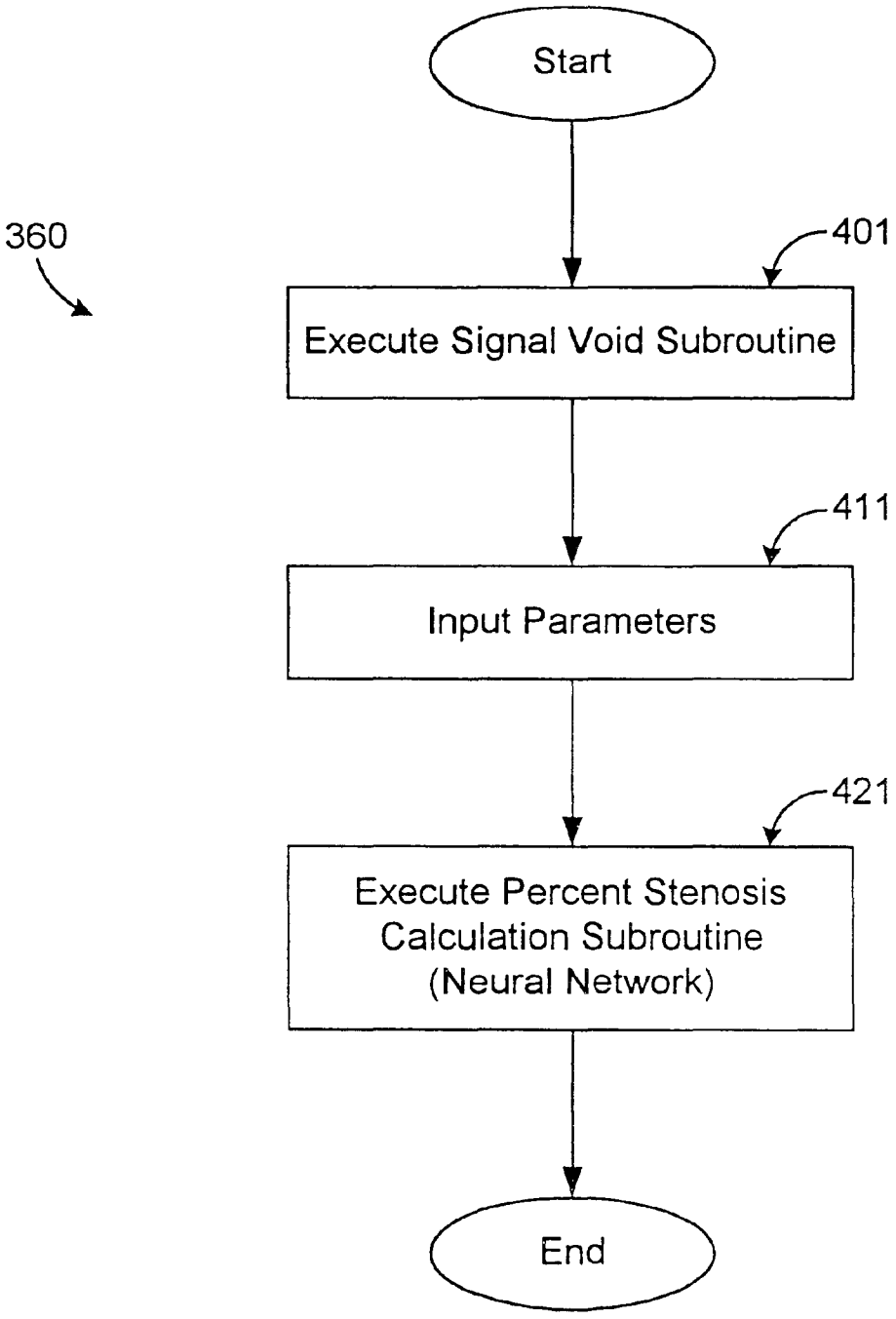
Start
360
401
Execute Signal Void Subroutine
411
Input Parameters
421
Execute Percent Stenosis Calculation Subroutine (Neural Network)
End

Fig. 4

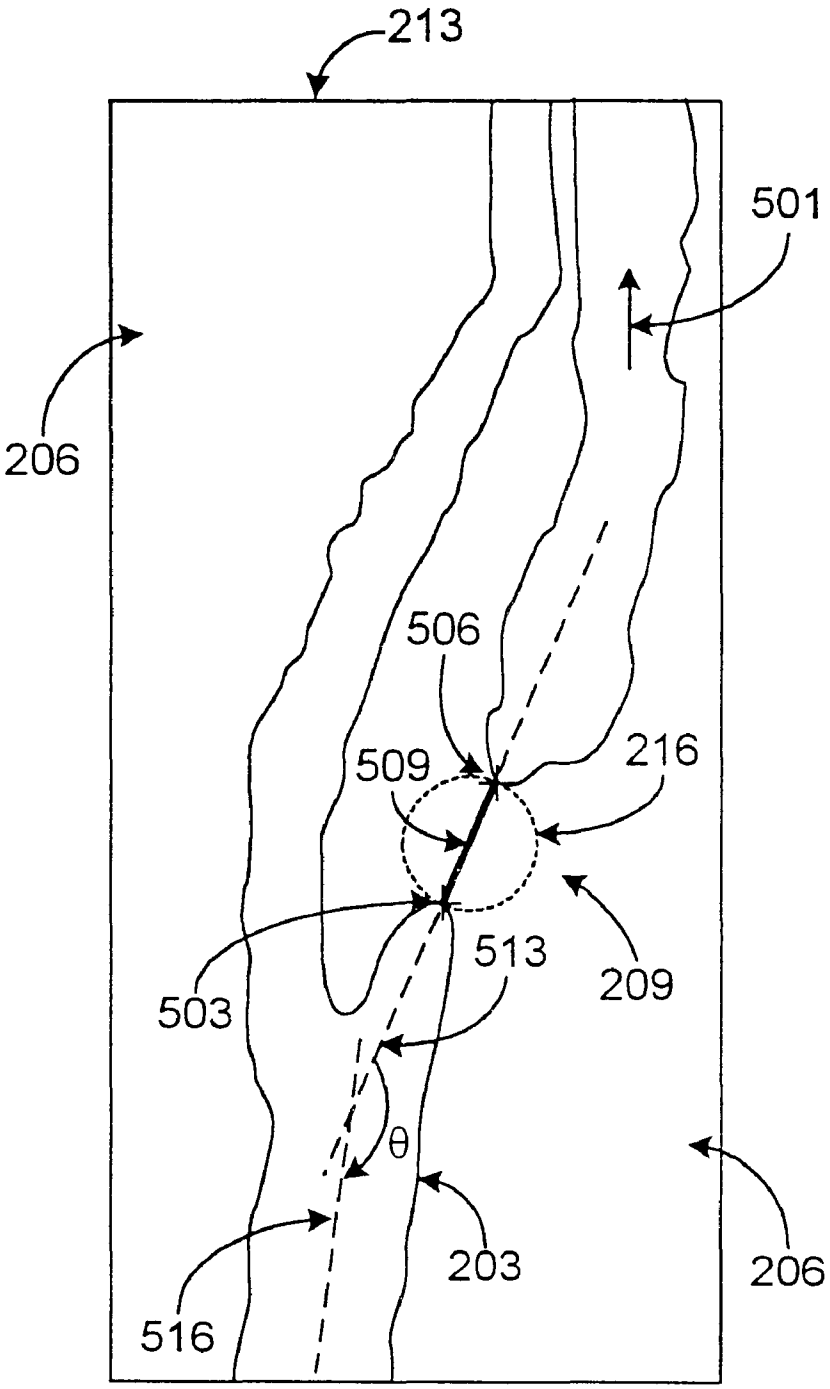

Fig. 5

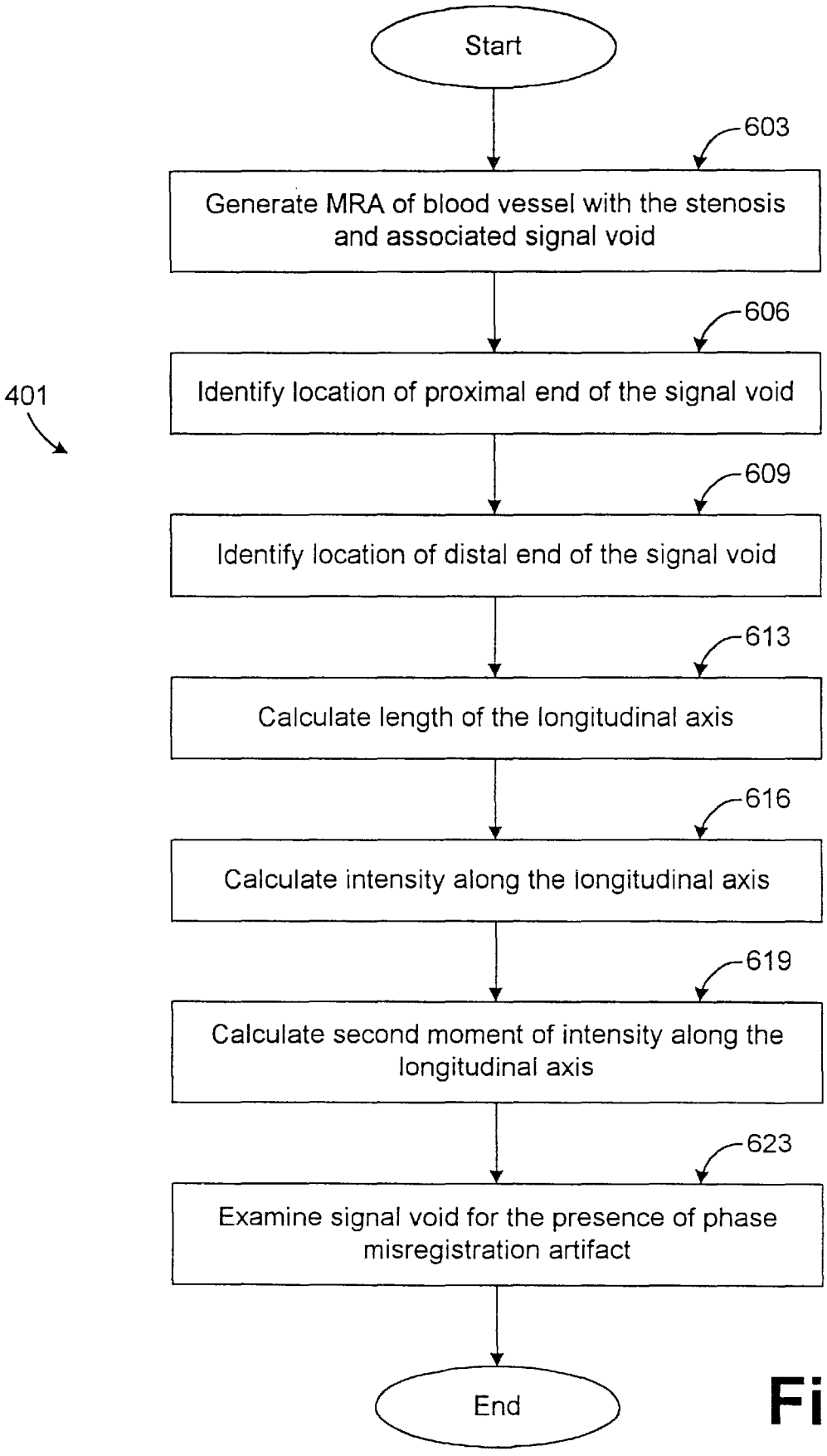
Start
603
Generate MRA of blood vessel with the stenosis and associated signal void
606
401
Identify location of proximal end of the signal void
609
Identify location of distal end of the signal void
613
Calculate length of the longitudinal axis
616
Calculate intensity along the longitudinal axis
619
Calculate second moment of intensity along the longitudinal axis
623
Examine signal void for the presence of phase misregistration artifact
End

Fig. 6

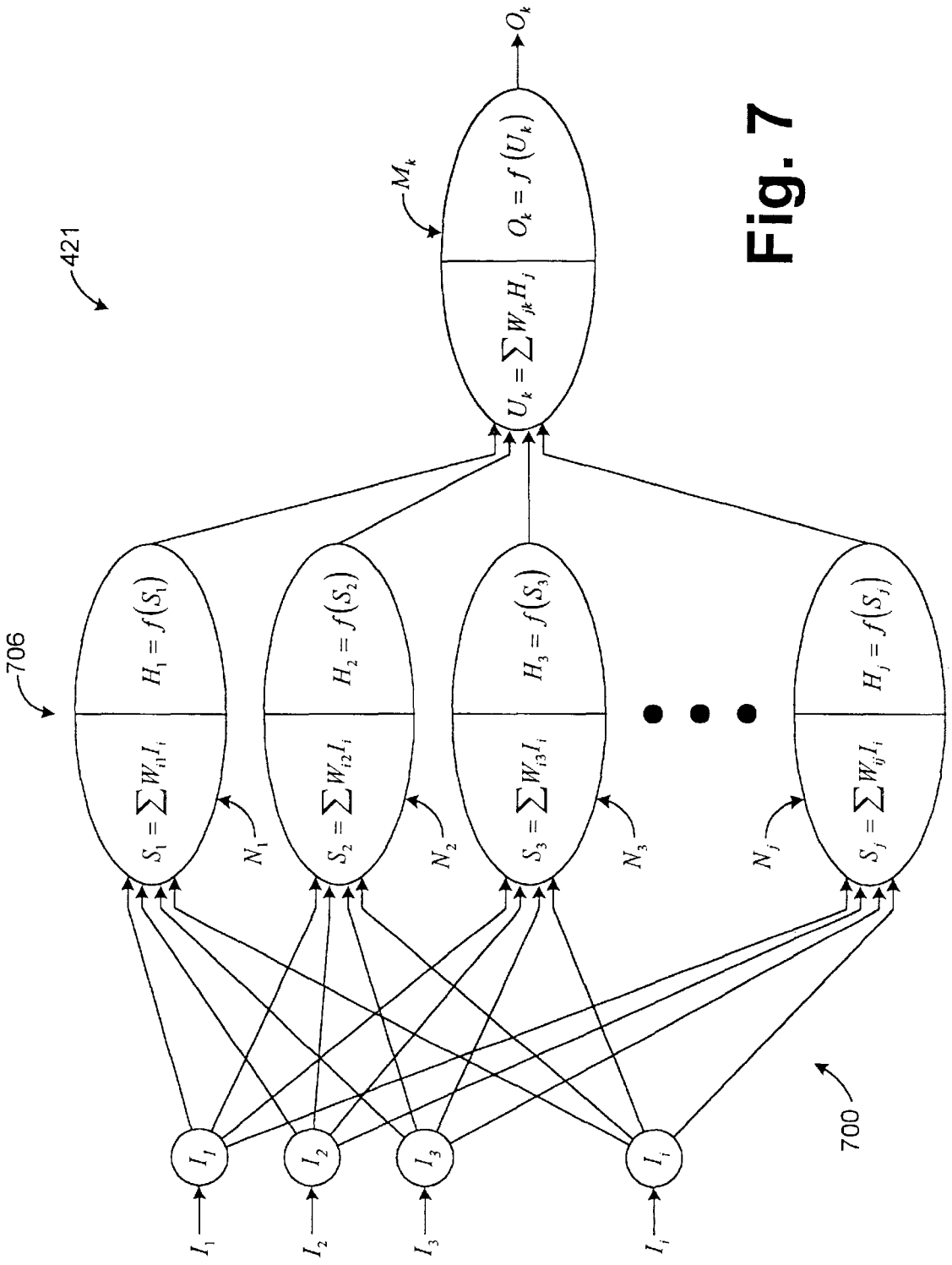
421
706
700
O_k
M_k
$O_k = f(U_k)$
$U_k = \sum W_{jk} H_j$
$H_1 = f(S_1)$
$H_2 = f(S_2)$
$H_3 = f(S_3)$
$H_j = f(S_j)$
$S_1 = \sum W_{i1} I_i$
$S_2 = \sum W_{i2} I_i$
$S_3 = \sum W_{i3} I_i$
$S_j = \sum W_{ij} I_i$
N_1
N_2
N_3
N_j
I_1
I_2
I_3
I_i

Fig. 7

SYSTEM AND METHOD FOR ANALYZING A MEDICAL IMAGE

CROSS-REFERENCE TO RELATED APPLICATIONS

This application claims priority to copending U.S. provisional patent application entitled "Knowledge Based Medical Image Analysis" filed on Mar. 20, 1998, and accorded serial No. 60/078,811, which is entirely incorporated herein by reference.

STATEMENT REGARDING FEDERALLY SPONSORED RESEARCH AND DEVELOPMENT

The U.S. Government has a paid-up license in this invention and the right in limited circumstances to require the patent owner to license others on reasonable terms as provided for by the terms of Contract No. HL-39437-06A2 awarded by the National Institute of Health.

TECHNICAL FIELD

The present invention is generally related to the field of analysis of a medical image, and, more particularly, is related to a system and method for analyzing a magnetic resonance image of stenosis in blood vessels.

BACKGROUND OF THE INVENTION

Atherosclerosis, the primary cause of heart attack and stroke, is currently responsible for most of the deaths in the Western world. In the United States alone, five million people seek treatment for cardiovascular ailments every year. Several symptoms indicate the need for surgical intervention to alleviate atherosclerotic disease. Some examples of these symptoms are transient ischemic attacks, physical performance on a treadmill stress test, and the existence of a prior incident of artery blockage or narrowing. A particular quantity that has been extensively studied and correlated to the proper clinical treatment is the degree of artery narrowing that is called the "percent stenosis".

Stenoses limit blood flow by raising the resistance to flow through the vessel. For example, the consequence of the stenosis in the cerebral circulation, where there is otherwise little resistance to flow, is that a significant stenosis can reduce the flow to the brain through that artery. In severe stenosis, a negative transmural pressure may be generated via the Bernoulli effect. If this occurs cyclically with the pulse, a stenosis may suddenly fracture because of mechanical fatigue failure which results in free floating particles in the blood flow which may block subsequent lesser blood vessels and result in stroke or other similar occlusive occurrence.

Consistent with hemodynamics studies such as the North American Symptomatic Carotid Endartectomy Trial, clinical observations indicate that patients with stenosis of approximately 60% or greater are candidates for surgery to correct the blockage. Generally, there is significant risk in the surgical methods which is balanced against the risk of having an atherosclerotic event. Accurate quantification of the percent stenosis is therefore critical in maximizing the patient's outcome and in minimizing healthcare costs.

The task of quantifying the severity of atherosclerotic narrowing of blood vessels or percent stenosis is called angiography, which refers to the imaging blood vessels. The current most effective method of angiography employed to determine the percent stenosis is x-ray angiography. In x-ray

angiography, a catheter is used to deliver a contrast agent to an upstream location of the stenosis. While the contrast agent is released into the blood flow upstream of the stenosis, x-rays are taken of the stenosis and surrounding area. The contrast agent ensures that the outlines of the blood flow are revealed on the x-ray which indicates any narrowing of the blood vessel in question.

However, x-ray angiography has significant drawbacks. For example, the contrast agent is toxic to the kidneys and some patients can develop an allergic reaction. Also, merely catheterizing a patient may cause a stroke or heart attack. Additionally, complications may arise because the catheter insertion point into the artery can heal slowly which necessitates an overnight stay in the hospital overnight for observation, thereby incurring the associated costs.

Another prospective angiographic method employs magnetic resonance imaging (MRI) technology to generate a view of the region containing stenosis of a blood vessel. However, the images generated using MRI generally suffer from inaccuracies due to the movement of blood through the blood vessel and other reasons. Consequently, the precise percent stenosis is very difficult if not impossible to quantify in a given image and MRI angiography is not practical.

SUMMARY OF THE INVENTION

The present invention provides a system and method for determining a severity of a stenosis in a blood vessel depicted in a magnetic resonance imaging (MRI) data set. Briefly described, in architecture, the system comprises a neural network configured to calculate the severity of the stenosis in the blood vessel based upon a number of input parameters, and the input parameters including at least one characteristic of a signal void associated with the stenosis in the MRI data set.

The present invention can also be viewed as a method for determining a severity of a stenosis in a blood vessel depicted in a magnetic resonance imaging (MRI) data set. In this regard, the method can be broadly summarized by the following steps: identifying a number of input parameters, the input parameters including at least one characteristic of a signal void associated with the stenosis in the MRI data set, and calculating the severity of the stenosis in the blood vessel based upon the input parameters.

The present invention has numerous advantages, one of which is that the present invention allows the easy and cost efficient determination of a percent stenosis in a patient without invasive and high risk surgical procedures. Other advantages of the invention include the fact that it is simple in design, user friendly, robust and reliable in operation, efficient in operation, and easily implemented for mass commercial production.

Other features and advantages of the present invention will become apparent to one with skill in the art upon examination of the following drawings and detailed description. It is intended that all such additional features and advantages be included herein within the scope of the present invention.

BRIEF DESCRIPTION OF THE SEVERAL VIEWS OF THE DRAWINGS

The invention can be better understood with reference to the following drawings. The components in the drawings are not necessarily to scale, emphasis instead being placed upon clearly illustrating the principles of the present invention. Moreover, in the drawings, like reference numerals designate corresponding parts throughout the several views.

FIG. 1A is an illustration of a normal blood vessel;

FIG. 1B is an illustration of a blood vessel with stenosis;

FIG. 2 is a side by side comparison of an x-ray angiogram of a blood vessel with stenosis and a two dimensional image of the same blood vessel generated from a magnetic resonance imaging data set;

FIG. 3 is a block diagram of a system according to the present invention;

FIG. 4 is a flow chart of the image analysis software stored in memory and executed by the system of FIG. 3;

FIG. 5 is a magnetic resonance imaging angiogram generated by the image analysis software of FIG. 4;

FIG. 6 is a flow chart of a subroutine of the image analysis software of FIG. 4; and

FIG. 7 is a block diagram of a neural network executed in a subroutine of the image analysis software of FIG. 4.

DETAILED DESCRIPTION OF THE INVENTION

Turning to FIGS. 1A and 1B, shown are illustrations of a normal blood vessel **101** and an abnormal blood vessel **109** with stenosis **106**. The normal blood vessel **101** has a normal blood flow **103** that is not restricted. The abnormal blood vessel **103** has a constricted blood flow **113** due to the presence of the stenosis **106**. Many individuals develop the stenosis **106** resulting in atherosclerosis that may eventually cause death by a heart attack or stroke. The stenosis **106** may occur in any blood vessel in the human body, but is more commonly found in specific locations in particular blood vessels such as those in the heart, brain, legs, and kidneys as known in the medical field.

The severity of the stenosis **106** is characterized by a value known as the percent stenosis. The percent stenosis is determined by identifying a first diameter D_1 which is the normal diameter of the blood vessel **103** and a second diameter D_2 which is the diameter of the stenosis **106** at its most narrow point. Percent stenosis is calculated according to the following formula:

$$\text{Percent Stenosis} = D_1 - D_2 / D_1 \%.$$

Currently, treatment is recommended to relieve the stenosis **106** when the percent stenosis is approximately 60% or greater. See North American Symptomatic Carotid Endarterectomy Trial Collaborators, "Beneficial Effect of Carotid Endarteremcomy in Symptomatic Patients with High-Grade Carotid Stenosis. N Engl J Med 325:445–53 (1991), and Downing et al., "Flow Through a Compliant Stenotic Artery," Advances in Bioengineering, American Society of Mechanical Engineers Bioengineering Division, 26:137–140 (1993), the above cited references being incorporated herein by reference.

With reference to FIG. 2, shown is a side by side comparison of two images which are simplified black and white representations of gray scale images. The first image is an x-ray angiogram **201** of a blood vessel **203** and the surrounding tissue **206**. The blood vessel **203** is, for example, the common carotid artery that branches into two lesser arteries, although it is understood that the present invention applies to any blood vessel that may experience stenosis. One of the lesser arteries of the blood vessel **203** is partially blocked by stenosis **209**. The second image is a two dimensional representation of a magnetic resonance angiogram **213** ("MRA **213**") of the same blood vessel **203** generated from a magnetic resonance imaging data set. The magnetic resonance angiogram **213** is preferably taken at times between heart pulses during times of the least movement of the blood vessel **203** for the best images, although this is not absolutely necessary. See Tsuruda et al., "Artifacts Associated with Magnetic Resonance Neuroangiography", American Journal of Neuroradiology, 13:1411–1422 (1992) which is incorporated herein by reference. Note that the blood vessel has a branch angle θ between the common carotid artery and the lesser artery in which the stenosis **209** occurs. The branch angle θ may be important in analysis that is to be discussed.

Generally, the x-ray angiogram **201** of the blood vessel **203** provides a high degree of accuracy as to the actual extent of the stenosis **209**. In particular, the walls of the stenosis **209** are well defined thereby making it possible to easily calculate the percent stenosis. However, the accuracy of the x-ray angiogram **201** is obtained at great risk during an invasive surgical procedure as described in the background above.

In determining the precise dimensions of the stenosis **209**, the MRA **213** is problematic. In particular, in the general location of the stenosis **209** there is a signal void **216** which appears as a region with decreased relative image intensity in the gray scale image due to stenosis **209** in the blood vessel **203**. The image intensity refers to the intensity of the pixels of the gray scale image. It is quite difficult, if not impossible, to determine the precise percent stenosis due to the signal void **216** as opposed to the x-ray angiogram **201**. This is unfortunate because magnetic resonance angiography is a non-surgical, non-invasive procedure with virtually no risk to the patient and is performed at a cost that is far less than x-ray angiography.

Upon further investigation, however, it has been discovered that the signal void **216** may provide information from which the percent stenosis can be determined given other known factors. Thus, further discussion of the nature of the signal void **216** is deemed appropriate.

It has been determined that the signal void **216** occurs due to the inability of a magnetic resonance imaging device to accurately obtain information from random movement in the blood stream. Specifically, magnetic resonance imaging employs magnetic and electromagnetic fields to manipulate the protons of the particular subject under scrutiny in "slices". Based on the frequency of the electromagnetic fields applied, the protons in a particular slice emit a signal, which is acquired. The frequency of the excitation signal is proportional to the magnetic field strength. The magnetic field strength is altered such that the frequency varies with position in the slice. The protons emit a signal at the excitation frequency received. Consequently, the location of the protons along one dimension in a particular slice is determined by the frequency of the signal they emit. Their location in a second dimension is determined by phase shifts. A Fourier transform is performed on the information obtained and the subject is reconstructed into an image as is known in the art.

The protons present in the blood that courses through the stenosis **209** of the blood vessel **203** experience acceleration in the middle of the stenosis **209** and a degree of turbulence after the stenosis **209**, the degree of turbulence varying depending upon the percent stenosis and the actual physical dimensions of the stenosis **209**. The signal void **216** is created by various mechanisms related to the acceleration and turbulence. One of these mechanisms is intravoxel phase dispersion related to the acceleration and turbulence that causes random motion of the protons present in the blood. This randomization results in intravoxel phase dis-

persion with different phase shifts being obtained in a voxel, resulting in destructive interference that appears as the signal void **216** in the final image.

A second mechanism resulting in the signal void **216** is phase misregistration artifact, sometimes referred to as "ghosting" in the literature, which refers to the fact that the location of the protons present in the blood do not stay stationary due to the randomization. Consequently, from slice to slice variations in the flow field appear to be at different spatial frequencies. Note that phase misregistration artifact is not specific to the signal void **216** alone, but may appear in other locations outside the signal void **216** as well.

Thus, it has been found there is a correlation between turbulence, or random movement, of water molecules in blood and the nature and extent of the signal void **216**. Consequently, the size and nature of the signal void **216** provides information as to the anatomy or, particularly, the stenosis **209** which created it. Therefore, the signal void **216** can be seen as a signature of the stenosis **209**.

Referring to FIG. **3**, shown is a block diagram of a medical image analysis system **300** according to an embodiment of the present invention. The medical image analysis system **300** includes a computer system **303** which comprises a processor **306**, a random access memory (RAM) **309**, and a stationary data storage device **313**, all of which are coupled to a data bus **316**. The computer system **303** further comprises a video interface **319**, a number of input interfaces **323**, a modem **326**, a number of output interfaces **329**, and a mobile data storage device **333**, all of which are also coupled to the data bus **316**. The stationary data storage device **313** may include, for example, a hard drive, compact disk read only memory, or other similar device.

The medical image analysis system **300** also includes a display device **336** that is coupled to the data bus **316** via the video interface **319**. The display device **336** may be a cathode-ray tube, liquid crystal display screen, or like device. The medical image analysis system **300** also includes several input devices, namely, a keyboard **339**, a mouse **343**, and a microphone **346** which are all coupled to the data bus **316** via the various input interfaces **323**. In addition, the modem **326** is coupled to an external network **349** thus allowing the computer system to send and receive data via the external network **349**. The external network **349** may be, for example, the Internet or other similar network.

The medical image analysis system **300** may further include audio speakers **353** or other output devices that are coupled to the data bus **316** via the output interfaces **329**. The mobile data storage device **333** may be one of several such devices that allow storage of data on a mobile platform such as a floppy disk drive, compact disc drive, mobile hard drive, or other similar data storage device.

The medical image analysis system **300** also includes image analysis software **360** which are generally stored on the stationary data storage device **313** along with data **363**. When the medical image analysis system **300** is operational, pertinent portions of the image analysis software **360** are loaded into the RAM **309** and is executed by the processor **306**. During operation of the medical image analysis system **300**, the image analysis software **360** may access the data **363** stored on the stationary data storage device **313**, loading the data **363** into the RAM **309** for various purposes as will be discussed.

With reference to FIG. **4**, shown is a flow chart of the image analysis software **360**. The image analysis software **360** begins with block **401** in which a signal void subroutine is executed. In the signal void subroutine **401**, a two dimensional magnetic resonance angiogram (MRA) **213** (FIG. **2**) is generated of a blood vessel using magnetic resonance imaging data from a patient, and pertinent characteristics of the signal void **316** (FIG. **3**) and other image characteristics appearing in the image are determined therefrom. The MRA **213** is generated from a magnetic resonance image data set which is part of the data **363** (hereafter "MRI data **363**") that is stored on either the stationary data storage **313** (FIG. **3**), or on a portable platform such as a floppy disk, compact disk, or other like medium that is placed in the mobile data storage device **333** (FIG. **3**). Ultimately, the MRI data **363** set is loaded from one of these storage places into the RAM **309** (FIG. **3**) and manipulated by the processor in generating the MRA **213**.

Note that the MRI data **363** may also be transmitted to the image analysis system **300** (FIG. **3**) via the network **349** (FIG. **3**) and the modem **326** (FIG. **1**). This allows MRI data to be transmitted to the image analysis system **300** from almost any location where the patients are examined. Such MRI data is downloaded from the network **349** and stored on the stationary data storage device **313**, etc.

Next, in block **411**, additional parameters such as anatomic or other parameters associated with the particular patient are input into the image analysis system **300**. Such parameters may include, but are not limited to, the blood flow rate, the presence of recirculation flow streak, and the branch angle θ if there is a relevant bend in the blood vessel **203** (FIG. **2**). Note that the rate of blood flow through the vessel is preferably determined between heart pulses when blood flow is generally more constant, a period commonly referred to as diastole as discussed by Saloner et al., "MRA Studies of Arterial Stenosis: Improvements by Diastolic Acquisition", Magnetic Resonance in Medicine, vol. 31, no. 2, pp. 196–203, which is incorporated herein by reference. The actual rate of blood flow through the blood vessel in question may be determined using a technique called phase velocity mapping in which the flow rate of the blood is measured in a plane perpendicular to the blood vessel axis well distal to the signal void **216**. A discussion of phase velocity mapping may be found in Firmin et al., "The Application of Phase Shifts in NMR for Flow Measurement", Magnetic Resonance in Medicine, 14:230–241 (1990a), which is incorporated herein by reference. Finally, in block **421**, a percent stenosis calculation subroutine is executed in which the percent stenosis is calculated based upon the signal void characteristics and the physiology parameters, preferably using a neural network.

With reference to FIG. **5**, shown is the two dimensional MRA **213** which serves as an example of those that are generated in block **401** (FIG. **4**). The direction of the blood flow **501** is as indicated. Both a proximal end **503** and a distal end **506** of the signal void **216** are indicated with a longitudinal axis **509** formed therebetween. A first vessel axis **513** and a second vessel axis **516** run along the direction of the main portion and the branch portion of the blood vessel **203**, forming the branch angle θ therebetween. From the MRA **213**, various signal void characteristics can be determined. For example, the length of the longitudinal axis **509** and the intensity along the longitudinal axis **509** may be determined. In particular, the intensity provides useful information as to the extent of the underlying turbulence in the blood. In addition, the second moment of intensity along the longitudinal axis **509** with respect to the distal end is important as it provides the standard deviation of the turbulence.

Turning then, to FIG. **6**, shown is a flow chart of the signal void subroutine **401** in which the pertinent anatomic characteristics and image characteristics of the MRA **213** are

determined. Beginning with block **603**, the MRA **213** (FIG. **5**) of the blood vessel **203** (FIG. **5**) with stenosis **209** (FIG. **5**) is generated on the display device **336** (FIG. **3**) from MRI data **363** (FIG. **3**) which is preferably three dimensional data of the slices obtained from the patient. Specific software used to generate the MRA **213** may employ "maximum intensity projection" or other equivalent techniques as known by those skilled in the art and, consequently, is not discussed in detail herein. In cases where the blood vessel is straight, one may simply pick a single dimensional slice from the MRI data **363** from an oblique plane through the target blood vessel to use as the MRA **213**. Next, in block **606**, the proximal end **503** of the signal void **216** (FIG. **5**) is located and, in block **609**, the distal end **506** of the signal void **216** is located. Note that locating the proximal and distal ends **503** and **506** may be accomplished, for example, by manipulating the mouse **343** (FIG. **3**) so as to locate a point or cross on each location, where depressing a button of the mouse confirms the location. Thereafter, in block **613**, the length of the longitudinal axis **509** (FIG. **5**) formed between the proximal and distal ends **503** and **506** is plotted and the length of the longitudinal axis **509** is calculated. The length of the signal void **216** is an important signal void characteristic obtained from the MRA **213**.

Moving to block **616**, another signal void characteristic comprising the intensity of the signal void **216** along the longitudinal axis **509** is calculated. Thereafter, in block **619**, an addition signal void characteristic comprising the second moment or standard deviation of the intensity along the longitudinal axis **509** is calculated. The signal void subroutine **401** then examines the MRA **213** for an image characteristic comprising the presence of phase misregistration artifact in block **623**. The presence of phase misregistration artifact is noted with a logical zero for "no" and a logical one for "yes". Thereafter, the signal void subroutine **401** ends and the image analysis software **300** (FIG. **4**) reverts to block **411** (FIG. **4**).

With reference to FIG. **7**, shown is a functional block diagram of the percent stenosis calculation subroutine **421**. The percent stenosis calculation subroutine **421** preferably employs a neural network **700** which includes multiple inputs I_i that are applied to generate one or more outputs O_k. The neural network **700** includes several input nodes **703** to which the inputs I_i are applied. The inputs I_i are the signal void characteristics, image characteristics, and the anatomic parameters discussed previously. In the preferred embodiment, the specific signal void characteristics, image characteristics, and anatomic parameters applied as inputs I_i to the neural network **700** include the length of the longitudinal axis of the signal void **216** (FIG. **2**), the average image intensity along the longitudinal axis **509** (FIG. **5**), the second moment of image intensity along the longitudinal axis, the presence of phase misregistration artifact (0="no", 1="yes"), blood flow rate, presence of recirculation flow streak (0="no", 1="yes"), and the branch angle. Note however, the present invention is not limited to these inputs as other signal void characteristics, image characteristics, or anatomic parameters may be employed as well as discussed below.

The output O_k of the neural network **700** is preferably the percent stenosis in the blood vessel **203** (FIG. **5**). However, other outputs may be included such as a certainty value which, for example, may range from 0 to 1 thereby indicating the level of certainty that the percent stenosis is correct.

The neural network **700** also includes a hidden layer **706** that comprises multiple neurons N_j. It is understood that while only a single hidden layer **706** is shown, that there may be multiple hidden layers **706**, each with a predetermined number of neurons N_j. In a particular embodiment for example, a single hidden layer **706** was used with a total of four neurons employed with significant success and accuracy in determining the percent stenosis. The neural network **700** also includes at least one output node M_k that generates the output O_k. It is understood that there may be more than a single output node M_k if so desired.

In calculating an output O_k, the inputs I_i are applied to the input nodes **703** which thereafter supply a copy of the inputs I_i to each of the neurons N_j in the hidden layer **706**. Generally, the neurons N_j that are simplified versions of biological neurons, are capable of performing a simple mathematical task. The output of each neuron N_j is a nonlinear function of its inputs. Upon receiving the inputs I_i, the neurons N_j perform a summation S_j of a weighted multiplication of each input I_i defined by

$$S_j=\Sigma W_{ij}I_i$$

where W_{ij} is defined as the weighting factor associated with each respective input I_i. If the summation S_j reaches a saturation value of the neuron N_j, then the neuron N_j this "activated" and outputs a non-zero value. The neural output H_j is calculated using the neuron activation function f(x) which may be, for example, a hyperbolic tangent sigmoidal function or a linear ramp function. These neuron activation functions differ somewhat from the function of a biological neuron, which has an activation function that more closely resembles a step function. The neural output H_j of each neuron N_j is calculated by

$$H_j=f(S_j).$$

The outputs H_j are then applied to an output node M_k that performs a summation U_k of a weighted multiplication of each neural output H_j defined by

$$U_k=\Sigma W_{jk}H_j$$

where W_{jk} is the weighting factor associated with each respective neural output H_j. Finally, the output O_k is calculated as using the output node activation function f as function of the summation U_k, where

$$O_k=f(U_k).$$

The neural network **700** is a "feedforward" neural network in that each neuron N_i processes all of the inputs from a previous layer by accepting a weighted sum of these inputs. It is understood that other types of neural networks such as feedback neural networks may be employed as well, where the input of a neuron N_i is also one of that neuron's outputs.

Before the neural network **700** can be used to generate the output(s) O_k from the inputs I_i, the neural network **700** is trained to recognize patterns using supervised training methods known to those skilled in the art. Training is accomplished first by identifying a number of sets of training inputs I_i, or training input sets, each training input set having a corresponding desired output(s). During training, the neural network **700** is exposed to the training input sets, thereby generating a corresponding output(s). The corresponding output(s) O_k from the output node M_k is compared to the desired output(s) from each training input set. A mean-squared network error is then calculated between the corresponding and desired output(s) and thereafter, the neural network **700** adjusts its weighting factors W to minimize this error. The application of all of the training input sets to be

used in a given circumstance is called an epoch. Generally, several epochs occur before the neural network **700** is trained acceptably. This process is repeated with sets of known input(s)/outputs(s) until the mean-squared error of the output(s) is below a prescribed tolerance.

There are several techniques used to train a neural network **700** as known by those skilled in the art. The above discussion contemplates that any such method may be employed. Perhaps the most common method is termed backpropagation which is known in the art. Note also that the number of hidden layers **706** and the number of output nodes M_k may vary depending upon the number of training input sets that are available to train the neural network **700**. Generally, a more complex network should be trained with more training sets to provide accurate output values.

Note, other approaches that may be used to calculate the percent stenosis based on the various inputs discussed herein include other statistical methods which can be used to model the relationship between the various input parameters and the percent stenosis. These approaches may include, for example, traditional multivariate nonlinear regression, principal component analysis, and discriminant analysis. Due to the difficulty identifying needed assumptions about curve fitting for nonlinear regression and, generally, due to the nonlinear relationships between the input parameters and the percent stenosis, these alternative approaches may not perform as accurately as the neural network **700**, but may ultimately suffice.

The signal void characteristics and the anatomic parameters applied as inputs I_i to the neural network **700** may also include characteristics and parameters not discussed above. For example, additional anatomic parameters might include a curvature of the blood vessel and the diameter of the blood vessel in addition to other parameters. Note that a crude measurement of the curvature of a blood vessel may be obtained in a manner similar to that in which the branch angle θ is determined as discussed previously, although other methods may be employed as well. Also, for different blood vessels, different combinations of various signal void characteristics and anatomic parameters may be employed to obtain accurate output values.

In addition, the image analysis software **360** (FIG. **3**) of the present invention can be implemented in hardware, software, firmware, or a combination thereof. In the preferred embodiment(s), the image analysis software **360** is implemented in software or firmware that is stored in a memory and that is executed by a suitable instruction execution system.

The flow charts and functional block diagrams of FIGS. **4–7** shows the architecture, functionality, and operation of a possible implementation of the image analysis software **360**. In this regard, each block represents a module, segment, or portion of code, which comprises one or more executable instructions for implementing the specified logical function (s). It should also be noted that in some alternative implementations, the functions noted in the blocks may occur out of the order noted in FIGS. **4**, **6**, and **7**. For example, two blocks shown in succession in FIG. **4** may in fact be executed substantially concurrently or the blocks may sometimes be executed in the reverse order, depending upon the functionality involved, as will be further clarified hereinbelow.

The image analysis software **360**, which comprises an ordered listing of executable instructions for implementing logical functions, can be embodied in any computer-readable medium for use by or in connection with an instruction execution system, apparatus, or device, such as a computer-based system, processor-containing system, or other system that can fetch the instructions from the instruction execution system, apparatus, or device and execute the instructions. In the context of this document, a "computer-readable medium" can be any means that can contain, store, communicate, propagate, or transport the program for use by or in connection with the instruction execution system, apparatus, or device. The computer readable medium can be, for example but not limited to, an electronic, magnetic, optical, electromagnetic, infrared, or semiconductor system, apparatus, device, or propagation medium. More specific examples (a non-exhaustive list) of the computer-readable medium would include the following: an electrical connection (electronic) having one or more wires, a portable computer diskette (magnetic), a random access memory (RAM) (magnetic), a read-only memory (ROM) (magnetic), an erasable programmable read-only memory (EPROM or Flash memory) (magnetic), an optical fiber (optical), and a portable compact disc read-only memory (CDROM) (optical). Note that the computer-readable medium could even be paper or another suitable medium upon which the program is printed, as the program can be electronically captured, via for instance optical scanning of the paper or other medium, then compiled, interpreted or otherwise processed in a suitable manner if necessary, and then stored in a computer memory.

Other references which are deemed important to the present invention include: Perman et al., "Artifacts from Polsatile Flow in Magnetic Resonance Imaging", Journal of Computer Assisted Tomography, 10: 473–483 (1986); Siegel et al., "Computational Simulation of Turbulent Signal Loss in 2D Time-of-Flight Magnetic Resonance Angiograms", Magnetic Resonance in Medicine, 37: 609–614 (1997); Seigel et al., "Comparison of Phantom and Computer-Simulated Images of Flow in a Convergent Geometry: Implications for Improved Two Dimensional Magnetic Resonance Angiography", Journal of Magnetic Resonance Imaging, 5:677–683 (1995; Bradley et al., "The Appearance of Rapidly Flowing Blood on Magnetic Resonance Images", AJR, 143:1157–1174 (1984); Firmin et al., "The Application of Phase Shifts in NMR for Flow Measurement", Magnetic Resonance in Medicine, 14:230–241 (1990a); Armoni, A., "Use of Neural Networks in Medical Diagnosis", M. D. Computing, 15:100–104 (1998); Jain et al., "On Training Sample Size and Complexity of Artificial Neural Net Classifier", Informatica, vol. 3, no. 3, pp. 301–337 (1992); and Scarselli et al., "Universal Approximation Using Feedforward Neural Networks: A Survey of Some Existing Methods, and Some New Results", Neural Networks, vol. 11, no. 1, pp. 15–37, (1998), all of the above listed references being incorporated herein by reference.

Many variations and modifications may be made to the above-described embodiment(s) of the invention without departing substantially from the spirit and principles of the invention. All such modifications and variations are intended to be included herein within the scope of the present invention.

Therefore, having thus described the invention, the following is claimed:

1. A system for determining a severity of a stenosis in a blood vessel depicted in a magnetic resonance imaging (MRI) data set, comprising:

a neural network configured to calculate the severity of the stenosis in the blood vessel based upon a number of input parameters;

the input parameters including at least one characteristic of a signal void associated with the stenosis in the MRI data set; and

a signal void analyzer configured to identify the characteristic of the signal void in the MRI set, wherein the signal void analyzer includes a graphical display generator configured to generate a two dimensional image of the signal void from the MRI data set, and a graphical plotter configured to plot at least two points on the two dimensional image and to determine the length of a line between the two points.

2. The system of claim **1**, wherein the signal void analyzer further comprises:

an average image intensity calculator configured to determine an average image intensity along the line; and

a second moment calculator configured to determine a second moment of image intensity along the line.

3. The system of claim **1**, wherein the neural network is configured to calculate the severity of the stenosis based upon a flow rate of blood through the blood vessel.

4. The system of claim **1**, wherein the neural network is configured to calculate the severity of the stenosis based upon a length of a longitudinal axis of the signal void, an average image intensity along the longitudinal axis of the signal void, and a presence of phase misregistration artifact.

5. The system of claim **4**, wherein the phase misregistration artifact includes a first component from inside the signal void and a second component from outside the signal void.

6. The system of claim **1**, wherein the neural network is configured to calculate the severity of the stenosis based upon a length of a longitudinal axis of the signal void.

7. The system of claim **6**, wherein the neural network is configured to calculate the severity of the stenosis based upon an average image intensity along the longitudinal axis of the signal void.

8. The system of claim **6**, wherein the neural network is configured to calculate the severity of the stenosis based upon a second moment of image intensity along the longitudinal axis of the signal void.

9. The system of claim **1**, wherein the neural network is configured to calculate the severity of the stenosis based upon a presence of phase misregistration artifact.

10. The system of claim **1**, wherein the neural network is configured to calculate the severity of the stenosis based upon a presence of recirculation flow streak.

11. The system of claim **1**, wherein the neural network is configured to calculate the severity of the stenosis based upon a branch angle of the blood vessel.

12. The system of claim **1**, wherein the neural network is configured to calculate the severity of the stenosis based upon intravoxel phase dispersion.

13. The system of claim **1**, wherein the neural network is configured to calculate the severity of the stenosis based upon a diameter of the blood vessel.

14. The system of claim **1**, wherein the neural network is configured to calculate the severity of the stenosis based upon a curvature of the blood vessel.

15. The system of claim **1**, wherein the neural network is configured to calculate the severity of the stenosis based upon an axis of the blood vessel.

16. The system of claim **1**, wherein the neural network is configured to calculate the severity of the stenosis based upon a direction of blood flow.

17. The system of claim **1**, wherein the neural network is configured to calculate the severity of the stenosis based upon a standard deviation of the turbulence.

18. The system of claim **1**, wherein the neural network is feedforward.

19. The system of claim **1**, wherein the neural network is feedback.

20. A system for determining a severity of a stenosis in a blood vessel depicted in a magnetic resonance imaging (MRI) data set, comprising:

means for calculating the severity of the stenosis in the blood vessel based upon a number of input parameters;

the input parameters including at least one characteristic of a signal void associated with the stenosis in the MRI data set; and

an analyzer means for identifying a number of predetermined characteristics of the signal void in the MRI data set, wherein the analyzer means includes means for generating a two dimensional image of the signal void from the MRI data set, and means for plotting at least two points on the two dimensional image and to determine the length of a line between the two points.

21. The system of claim **20**, wherein the analyzer means further comprises:

means for determining an average image intensity along the line; and

means for determining a second moment of image intensity along the line.

22. The system of claim **20**, wherein the means for calculating the severity of the stenosis includes a means for calculating the severity of the stenosis based upon a flow rate of blood through the blood vessel.

23. The system of claim **20**, wherein the means for calculating the severity of the stenosis includes a means for calculating the severity of the stenosis based upon a length of a longitudinal axis of the signal void, an average image intensity along the longitudinal axis of the signal void, and a presence of phase misregistration artifact.

24. The system of claim **20**, wherein the phase misregistration artifact includes a first component from inside the signal void and a second component from outside the signal void.

25. The system of claim **20**, wherein the means for calculating the severity of the stenosis includes a means for calculating the severity of the stenosis based a presence of phase misregistration artifact.

26. The system of claim **20**, wherein the means for calculating the severity of the stenosis includes a means for calculating the severity of the stenosis based a presence of recirculation flow streak.

27. The system of claim **20**, wherein the means for calculating the severity of the stenosis includes a means for calculating the severity of the stenosis based upon a branch angle of the blood vessel.

28. The system of claim **20**, wherein the means for calculating the severity of the stenosis includes a means for calculating the severity of the stenosis based upon intravoxel phase dispersion.

29. The system of claim **20**, wherein the means for calculating the severity of the stenosis includes a means for calculating the severity of the stenosis based upon a diameter of the blood vessel.

30. The system of claim **20**, wherein the means for calculating the severity of the stenosis includes a means for calculating the severity of the stenosis based upon a curvature of the blood vessel.

31. The system of claim **20**, wherein the means for calculating the severity of the stenosis includes a means for calculating the severity of the stenosis based upon an axis of the blood vessel.

32. The system of claim **20**, wherein the means for calculating the severity of the stenosis includes a means for calculating the severity of the stenosis based upon a direction of blood flow.

33. The system of claim 20, wherein the means for calculating the severity of the stenosis includes a means for calculating the severity of the stenosis based upon a standard deviation of the turbulence.

34. The system of claim 20, wherein the neural network is feedforward.

35. The system of claim 20, wherein the neural network is feedback.

36. A method for determining a severity of a stenosis in a blood vessel depicted in a magnetic resonance imaging (MRI) data set, comprising the steps of:

identifying a number of input parameters, the input parameters including at least one characteristic of a signal void associated with the stenosis in the MRI data set, wherein the step of identifying the number of input parameters includes the step of determining a length of a longitudinal axis of the signal void, an average image intensity along the longitudinal axis of the signal void, and a presence of phase misregistration artifact; and

calculating the severity of the stenosis in the blood vessel based upon the input parameters.

37. The method of claim 36, wherein the step of identifying the number of parameters further includes the step of determining an intravoxel phase dispersion.

38. The method of claim 36, wherein the step of identifying the number of parameters further includes the step of determining a diameter of the blood vessel.

39. The method of claim 36, wherein the step of identifying the number of parameters further includes the step of determining a curvature of the blood vessel.

40. The method of claim 36, wherein the step of identifying the number of parameters further includes the step of determining a axis of the blood vessel.

41. The method of claim 36, wherein the step of identifying the number of parameters further includes the step of determining a direction of blood flow.

42. The method of claim 36, wherein the step of identifying the number of parameters further includes the step of determining a standard deviation of the turbulence.

43. The method of claim 36, wherein the step of calculating the severity of the stenosis is accomplished with a feedforward neural network.

44. The method of claim 36, wherein the step of calculating the severity of the stenosis is accomplished with a feedback neural network.

45. The method of claim 36, wherein the step of identifying the number of parameters further includes the step of determining a second moment of intensity along the longitudinal axis of the signal void.

46. The method of claim 36, wherein the step of calculating the severity of the stenosis is accomplished with a traditional multivariate nonlinear regression.

47. The method of claim 36, wherein the step of calculating the severity of the stenosis is accomplished with a principal component analysis.

48. The method of claim 36, wherein the step of calculating the severity of the stenosis is accomplished with a discriminant analysis.

49. The method of claim 36, wherein the phase misregistration artifact includes a first component from inside the signal void and a second component from outside the signal void.

50. A method for determining a severity of a stenosis in a blood vessel depicted in a magnetic resonance imaging (MRI) data set, comprising the steps of:

identifying a number of input parameters, the input parameters including at least one characteristic of a signal void associated with the stenosis in the MRI data set, wherein the step of identifying the number of input parameters further includes the step of determining a length of a longitudinal axis of the signal void and the step of determining a flow rate of blood through the blood vessel; and

calculating the severity of the stenosis in the blood vessel based upon the input parameters.

51. The method of claim 50, wherein the step of identifying the number of parameters further includes the step of determining an intravoxel phase dispersion.

52. The method of claim 50, wherein the step of identifying the number of parameters further includes the step of determining a diameter of the blood vessel.

53. The method of claim 50, wherein the step of identifying the number of parameters further includes the step of determining a curvature of the blood vessel.

54. The method of claim 50, wherein the step of identifying the number of parameters further includes the step of determining a axis of the blood vessel.

55. The method of claim 50, wherein the step of identifying the number of parameters further includes the step of determining a direction of blood flow.

56. The method of claim 50, wherein the step of identifying the number of parameters further includes the step of determining a standard deviation of the turbulence.

57. The method of claim 50, wherein the step of calculating the severity of the stenosis is accomplished with a feedforward neural network.

58. The method of claim 50, wherein the step of calculating the severity of the stenosis is accomplished with a feedback neural network.

59. The method of claim 50, wherein the step of identifying the number of parameters further includes the step of determining a second moment of intensity along the longitudinal axis of the signal void.

60. The method of claim 50, wherein the step of calculating the severity of the stenosis is accomplished with a traditional multivariate nonlinear regression.

61. The method of claim 50, wherein the step of calculating the severity of the stenosis is accomplished with a principal component analysis.

62. The method of claim 50, wherein the step of calculating the severity of the stenosis is accomplished with a discriminant analysis.

63. A method for determining a severity of a stenosis in a blood vessel depicted in a magnetic resonance imaging (MRI) data set, comprising the steps of:

identifying a number of input parameters, the input parameters including at least one characteristic of a signal void associated with the stenosis in the MRI data set, and wherein the step of identifying the number of input parameters further includes the step of determining an average image intensity along the longitudinal axis and the step of determining a flow rate of blood through the blood vessel; and

calculating the severity of the stenosis in the blood vessel based upon the input parameters.

64. A method for determining a severity of a stenosis in a blood vessel depicted in a magnetic resonance imaging (MRI) data set, comprising the steps of:

identifying a number of input parameters, the input parameters including at least one characteristic of a signal void associated with the stenosis in the MRI data set, wherein the step of identifying the number of input parameters includes the steps of, generating a two dimensional image of the signal void from the MRI

data set, and plotting at least two points on the two dimensional image and to determine the length of a line between the two points; and

calculating the severity of the stenosis in the blood vessel based upon the input parameters.

65. The method of claim **64**, wherein the step of identifying the predetermined characteristics of the signal void further comprises the steps of:

determining an average image intensity along the line; and

determining a second moment of image intensity along the line.

66. The method of claim **64**, wherein the step of identifying the number of parameters further includes the step of determining an intravoxel phase dispersion.

67. The method of claim **64**, wherein the step of identifying the number of parameters further includes the step of determining a diameter of the blood vessel.

68. The method of claim **64**, wherein the step of identifying the number of parameters further includes the step of determining a curvature of the blood vessel.

69. The method of claim **64**, wherein the step of identifying the number of parameters further includes the step of determining a axis of the blood vessel.

70. The method of claim **64**, wherein the step of identifying the number of parameters further includes the step of determining a direction of blood flow.

71. The method of claim **64**, wherein the step of identifying the number of parameters further includes the step of determining a standard deviation of the turbulence.

72. The method of claim **64**, wherein the step of calculating the severity of the stenosis is accomplished with a feedforward neural network.

73. The method of claim **64**, wherein the step of calculating the severity of the stenosis is accomplished with a feedback neural network.

74. The method of claim **64**, wherein the step of identifying the number of parameters further includes the step of determining a second moment of intensity along the longitudinal axis of the signal void.

75. The method of claim **64**, wherein the step of calculating the severity of the stenosis is accomplished with a traditional multivariate nonlinear regression.

76. The method of claim **64**, wherein the step of calculating the severity of the stenosis is accomplished with a principal component analysis.

77. The method of claim **64**, wherein the step of calculating the severity of the stenosis is accomplished with a discriminant analysis.

78. A system for determining a severity of a stenosis in a blood vessel depicted in a magnetic resonance imaging (MRI) data set, comprising:

a neural network configured to calculate the severity of the stenosis in the blood vessel based upon a number of input parameters;

the input parameters including at least one characteristic of a signal void associated with the stenosis in the MRI data set; and

a signal void analyzer configured to identify the characteristic of the signal void in the MRI set, the signal void analyzer configured to determine a longitudinal axis of the signal void, the signal void analyzer configured to determine an average image intensity along the longitudinal axis of the signal void, the signal void analyzer configured to determine a presence of phase misregistration artifact.

79. A system for determining a severity of a stenosis in a blood vessel depicted in a magnetic resonance imaging (MRI) data set, comprising:

a neural network configured to calculate the severity of the stenosis in the blood vessel based upon a number of input parameters;

the input parameters including at least one characteristic of a signal void associated with the stenosis in the MRI data set; and

a signal void analyzer configured to identify the characteristic of the signal void in the MRI set, the signal void analyzer configured to determine a longitudinal axis of the signal void, the signal void analyzer configured to determine a flow rate of blood through the blood vessel.

80. A system for determining a severity of a stenosis in a blood vessel depicted in a magnetic resonance imaging (MRI) data set, comprising:

a neural network configured to calculate the severity of the stenosis in the blood vessel based upon a number of input parameters;

the input parameters including at least one characteristic of a signal void associated with the stenosis in the MRI data set; and

a signal void analyzer configured to identify the characteristic of the signal void in the MRI set, the signal void analyzer configured to determine an average image intensity along a longitudinal axis of the signal void, the signal void analyzer configured to determine a flow rate of blood through the blood vessel.

* * * * *

UNITED STATES PATENT AND TRADEMARK OFFICE

CERTIFICATE OF CORRECTION

PATENT NO. : 6,377,832 B1
DATED : April 23, 2002
INVENTOR(S) : Bergman et al.

It is certified that error appears in the above-identified patent and that said Letters Patent is hereby corrected as shown below:

Column 3,
Line 23, after "vessel", delete "109" and replace it with -- 103 --
Line 25, after "flow," delete "103" and replace it with -- 109 --

Column 6,
Line 3, delete "316 (FIG. 3)" and replace it with -- 216 (FIG. 2) --

Signed and Sealed this

Twenty-ninth Day of October, 2002

Attest:

JAMES E. ROGAN
Director of the United States Patent and Trademark Office

Attesting Officer